Current Science
CS 5 (5), 4561-4571 (2025)
Received 20 June 2025 | **Revised 18 July** 2025 | **Accepted 15 August** 2025 | **Online Available 23 September** 2025
https://doi.org0/10.52845/CS/2025-5-5-20

Current Science

Current Science

OPEN ACCESS

ISSN(O)2795-8639

Review Article

Expression Profile of CDC45 as a Potential Therapeutic Target in HPV-Associated Cervical Cancer and Pan-Cancer Prognostic Heterogeneity

Mei Qin[1], Bing Li[2], Xupeng Chen[3], Xi He[1,*], Xian Zhu[4,*]

[1]Department of Gynaecology, Zhuzhou Central Hospital, Zhuzhou, Hunan, 412000, China

[2]Department of Ultrasound, Zhuzhou Central Hospital, Zhuzhou, Hunan, 412000, China

[3]Department of Laboratory, Zhuzhou Central Hospital, Zhuzhou, Hunan, 412000, China

[4]Department of Nuclear Medicine, Zhuzhou Central Hospital, Zhuzhou, Hunan, 412000, China

[*]Corresponding Author: Xi He, Xian Zhu

Abstract:

Objective: This study aimed to elucidate the expression profile, clinical relevance, and mechanistic role of cell division cycle protein 45 (CDC45) in cervical carcinoma (CC) pathogenesis, while assessing its pan-cancer prognostic significance.

Methods: Multi-cohort transcriptomic analysis of CDC45 was performed using TCGA-CESC (306 tumors, 18 normal), GEO datasets (GSE63514: 152 samples; GSE67522: 42 samples), and experimental validation with 4 clinical CC/normal pairs. In addition, CDC45 expression and human papilloma virus (HPV) positivity and negativity were analyzed in CC, oral squamous cell carcinoma (OSCC), head and neck squamous cell carcinoma (HNSCC) from GEO database (GSE39001-CESCC, GSE67522-CESCC, GSE40774-HNSCC, GSE55542-OSCC). Differential expression, survival correlations, and pathway enrichment (GSEA) were analyzed. A prognostic nomogram integrating CDC45 expression and clinical variables was developed. Pan-cancer profiling across 34 malignancies (TCGA/TARGET/GTEx, N=19,131) evaluated CDC45's prognostic utility.

Results: CDC45 was significantly overexpressed in CC tissues versus normal (TCGA: $p<0.0001$; GEO: $p<0.0001$), validated experimentally (mRNA: $p<0.01$; protein: $p<0.05$). HPV-positive CC, OSCC, and HNSCC exhibited higher CDC45 levels than HPV-positive/negativity samples (CC: $p<0.0001$; OSCC: $p<0.01$; HNSCC: $p<0.001$). GSEA revealed CDC45's association with DNA repair (mismatch/homologous recombination), replication, and cell cycle pathways (FDR<0.25). High CDC45 expression correlated with prolonged overall survival (HR=0.58, $p=0.022$) and progression-free survival (HR=0.56, $p=0.016$). A nomogram incorporating CDC45 and p-TNM stage (I vs IV) status predicted 1-/3-/5-year survival (C-index=0.702). Pan-cancer analysis identified CDC45 as a dual-context prognostic marker: high expression conferred poor survival in glioblastoma, renal/liver cancers (HR>1, $p<0.05$), while low expression predicted adverse outcomes in ovarian/lymphoid malignancies (HR<1, $p<0.05$).

Conclusion: CDC45 overexpression in CC is linked to HPV-driven carcinogenesis, genomic instability, and replication stress, serving as an independent prognostic indicator. Its pan-cancer dichotomy underscores tissue-specific oncogenic roles. These findings nominate CDC45 as a potential therapeutic target and predictive biomarker for cervical and other malignancies.

Keywords: Cervical carcinoma, Cell division cycle protein 45, Human papilloma virus, Pan-Cancer, Prognosis

1. Introduction

Cervical carcinoma (CC) remains a critical global health challenge as the second most prevalent gynecologic malignancy, accounting for substantial morbidity and mortality worldwide [1]. Contemporary epidemiological analyses reveal an escalating incidence trajectory in developing nations, particularly among younger cohorts [2]. In China alone, 2022 surveillance data documented 119,300 new diagnoses and 37,200 CC-related fatalities [3], paralleling the 13,960 projected cases and 4,310 deaths reported in the United States for 2023 [4]. Persistent infection with high-risk human papillomavirus (HPV) subtypes, notably HPV16/18, drives over 70% of cervical malignancies through dysregulation of tumor suppressor pathways [5-6]. Despite advances in early detection and therapeutic strategies, approximately 20-30% of patients experience disease recurrence, with metastatic CC demonstrating a dismal 5-year survival rate below 20% [7-8].

Emerging evidence implicates replication stress-induced genomic instability as a hallmark of cancer progression [9]. Central to this process is Cell Division Cycle 45 (CDC45), an indispensable eukaryotic helicase component required for replication fork initiation and stabilization [10]. Unlike other replication licensing factors, CDC45 exhibits non-redundant functionality in maintaining replication fidelity through helicase activation [11]. Clinically, CDC45 overexpression has been mechanistically linked to accelerated cell cycle progression in multiple malignancies, including hepatocellular carcinoma and triple-negative breast cancer, where it correlates with advanced staging and reduced overall survival [12-13]. Notably, CDC45 serves as a downstream effector of c-Myc oncogenic signaling, recapitulating replication stress phenotypes characteristic of Myc-driven tumorigenesis [14]. While preliminary studies suggest CDC45's potential as a pan-cancer biomarker [15], its functional role and prognostic relevance in CC pathogenesis remain poorly characterized.

This investigation systematically evaluates CDC45's expression profile and clinical associations in CC through multi-cohort analysis while extending to pan-cancer contexts. Our findings aim to elucidate CDC45's mechanistic contributions to cervical carcinogenesis and establish its utility as a therapeutic vulnerability.

1. Methods and Materials

2.1 Data Collection and Workflow

2.1 Data Acquisition and Processing Pipeline

Transcriptomic profiles of CDC45 and associated clinicopathological records for cervical carcinoma (CC) were retrieved from three repositories: TCGA portal, GEO datasets GSE63514 (accession code: GSE63514), and GSE67522 (accession code: GSE67522). The TCGA cohort comprised 306 malignant specimens and 18 non-neoplastic cervical tissues. GSE63514 contained 152 clinical samples (24 normal, 15 low-grade intraepithelial lesions, and 113 high-grade/CC specimens), while GSE67522 included 42 samples (20 HPV-positive CC and 22 normal tissues with 50% HPV positivity). Supplementary validation involved 4 paired tumor-adjacent normal specimens from Zhuzhou Central Hospital (Ethics approval: 20231046). Figure 1 delineates the integrative analytical framework.

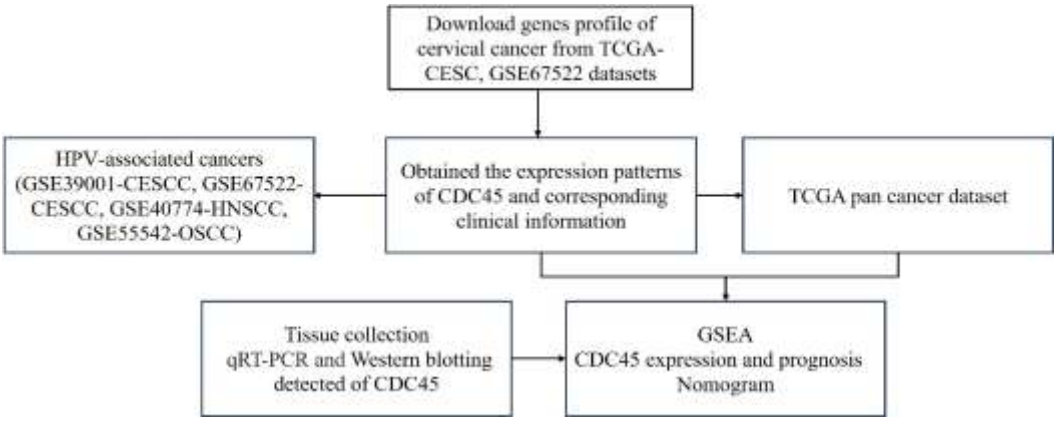

Figure 1, Workflow of the study.

2.2 Transcriptional Profiling of CDC45

Differential expression patterns of CDC45 across cohorts were evaluated using the clusterProfiler R toolkit. Specimens were dichotomized into high/low expression cohorts via median cutoff stratification. Survival outcomes (overall survival [OS], event status) were correlated with expression levels through Kaplan-Meier analysis, with TCGA serving as the principal validation platform.

2.3 Pathway Enrichment Profiling

Gene Set Enrichment Analysis (GSEA v3.0, https://www.gsea-msigdb.org/gsea/index.jsp) was implemented to delineate CDC45-associated molecular pathways. Samples were partitioned into tertiles (high: top 50%; low: bottom 50%) using the Kyoto Encyclopedia of Genes and Genomes (KEGG) reference set (c2.cp.kegg.v7.4). Significance thresholds were established as permutation count=1000, gene set size=5-5000, nominal $P<0.05$, and false discovery rate (FDR)<0.25.

2.4 Nomogram

Cox proportional hazards regression identified CDC45 expression, age, histologic grade, and pathologic TNM stage as independent prognostic determinants in TCGA-CESC. These covariates were integrated into a predictive nomogram using the rms R package. Model discrimination for 1-/3-/5-year survival was quantified through time-dependent ROC analysis, with area under the curve (AUC) calculated at each timepoint.

Internal validation employed 1000 bootstrap resamples to compute Harrell's concordance index (C-index) and generate calibration plots comparing predicted versus observed outcomes. Continuous nomogram refinement was guided by likelihood ratio tests and Akaike information criterion (AIC) optimization.

2.5 Tissue Collection

Four CC/ cancer adjacent tissue pairs were cryopreserved (-80°C) following ethical procurement (Zhuzhou Central Hospital, No. 2023 1046) for immunohistochemical validation. Informed consent was obtained per Declaration of Helsinki guidelines.

2.6 Quantitative Reverse Transcription Polymerase Chain Reaction and Western Blotting

Quantitative reverse transcription polymerase chain reaction (qRT-PCR): CDC45 transcript levels were assessed using SYBR Green chemistry (TB Green Premix Ex Taq™, Takara Bio RR036A). Total RNA from 50 mg cervical specimens (tumor/normal pairs) was isolated with TRIzol™ (Invitrogen) via mechanical homogenization (KZ-III-FP, Servicebio). RNA integrity (RIN >7.0) was validated prior to reverse transcription using PrimeScript™ RT Master Mix (Takara Bio) under manufacturer-specified conditions (37°C/15 min→85°C/5 sec). Primer pairs (Table 1) designed through NCBI Primer-BLAST underwent melt curve validation. Amplifications (20 μL triplicates) on QuantStudio 5 (Applied Biosystems) followed: 95°C/30 sec initiation; 40 cycles of 95°C/5 sec denaturation and 60°C/30 sec annealing/extension.

Table 1, RT-PCR primer information

Gene name	Primer sequence (5'- 3')
H-β-actin-F	GAGCACAGAGCCTCGCCTTT
H-β-actin-R	TCATCATCCATGGTGAGCTGG
H-CDC45-F	TTCGTGTCCGATTTCCGCAAA
H-CDC45-R	TGGAACCAGCGTATATTGCAC

Western Blotting: Cervical tissue lysates were homogenized in RIPA/protease inhibitor cocktail using a cryogenic grinder (KZ-III-F). Protein quantification employed BCA assay with BSA calibration. Samples (40 μg/lane) underwent SDS-PAGE (5% stacking gel/50 V; 12% resolving gel/120 V) until dye-front migration. Proteins were transferred to PVDF membranes (100 V, 60-90 min) followed by 1 h blocking in 5% milk-TBST. Membranes were incubated with primary antibodies (CDC45 1:1000, β-actin 1:5000) at 4°C overnight, then HRP-secondaries (1:5000) for 1 h at 25°C. Signals were developed with ECL Prime and quantified via chemiluminescence imaging (JS-1070P/IPWIN60), normalized to β-actin.

2.7 Analysis CDC45 of Expression and Prognosis in Pan-Cancer

CDC45 expression landscapes across 34 malignancies were interrogated using harmonized transcriptomic data from TCGA, TARGET, and GTEx cohorts (N=19,131; G=60,499) accessed via UCSC Xena Browser. Clinicogenomic variables including overall survival (OS) status and CDC45 expression levels were extracted per tumor type (Supplementary Table 2). Cohort stratification employed median-centered CDC45 expression thresholds (high vs. low). Survival disparities between expression subgroups were assessed through Kaplan-Meier methodology using the survival R package (v3.2-3). Log-rank tests determined statistical significance, with hazard ratios (HR) calculated via Cox proportional hazards models.

2.8 Statistical Analysis

Analyses were conducted in R 4.0.3 and GraphPad Prism 9.3.1. Intergroup comparisons employed Student's t-test with α=0.05 significance threshold. Resampling methods ensured reproducibility across all models.

Results:

3.1 The Expression of CDC45 in Cervical Cancer

CDC45 was significantly overexpressed in CC tissues compared to normal controls across both the TCGA-CESC and GSE67522 datasets (all $p < 0.0001$; Figures 2A-B). Consistent with these bioinformatics findings, experimental validation via quantitative PCR (qPCR) and Western blot analyses of fresh CC tissues and paired adjacent non-tumor tissues confirmed elevated CDC45 expression at the mRNA ($p < 0.01$) and protein levels ($p < 0.05$), respectively (Figures 2C-F).

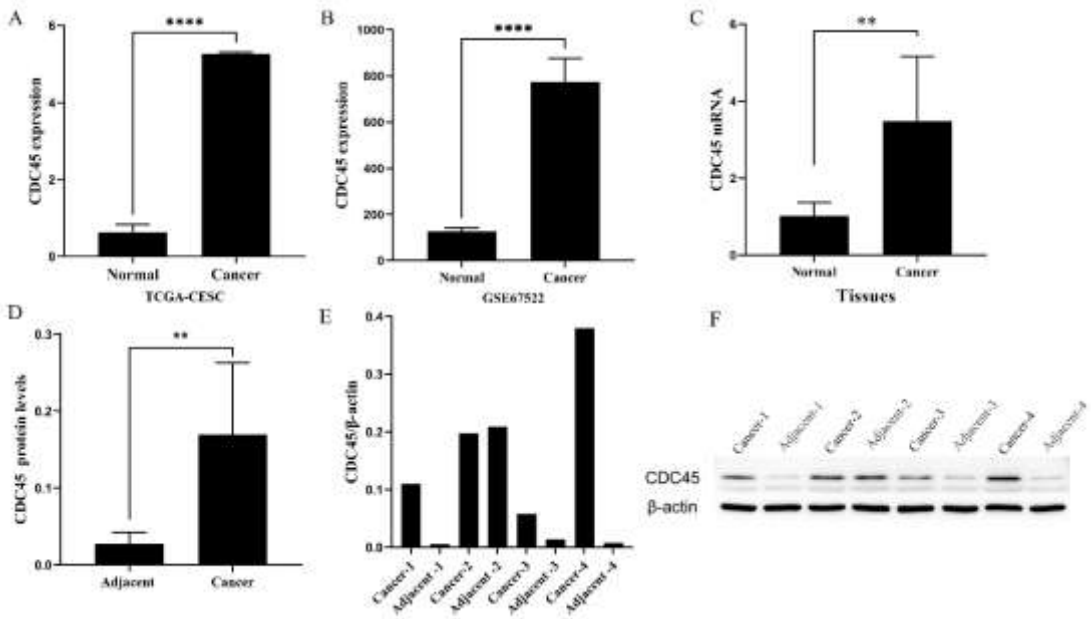

Figure 2, Expression of CDC45 in CC. (A–B) CDC45 was overexpressed in CC tissues in the TCGA-CESC and GSE67522 datasets. (C–F) mRNA and protein expression levels of CDC45 in CC and adjacent normal tissues. (, $p < 0.01$; ****, $p < 0.0001$).**

3.2 CDC45 Expression in HPV Infected Tumors

The expression of CDC45 was analyzed of HPV positive and HPV negative in oral squamous cell carcinoma (OSCC), head and neck squamous cell carcinoma (HNSCC), and cervical squamous cell carcinoma (CSCC). In CC, the expression of CDC45 was significantly higher in HPV-positive tissues than in HPV-positive normal cervical tissues ($p < 0.0001$, Figure 3 A-B). However, there was no difference in the expression of CDC45 between HPV positive and HPV negative normal cervical tissues. In HNSCC, CDC45 is significantly overexpressed in HPV positive samples compared to HPV negative samples ($p < 0.001$, Figure 3 C). In OSCC (Figure 3 D), CDC45 was significantly overexpressed in HPV active samples ($p<0.01$), while there was no

difference between HPV negative and HPV active samples (p＞0.05).

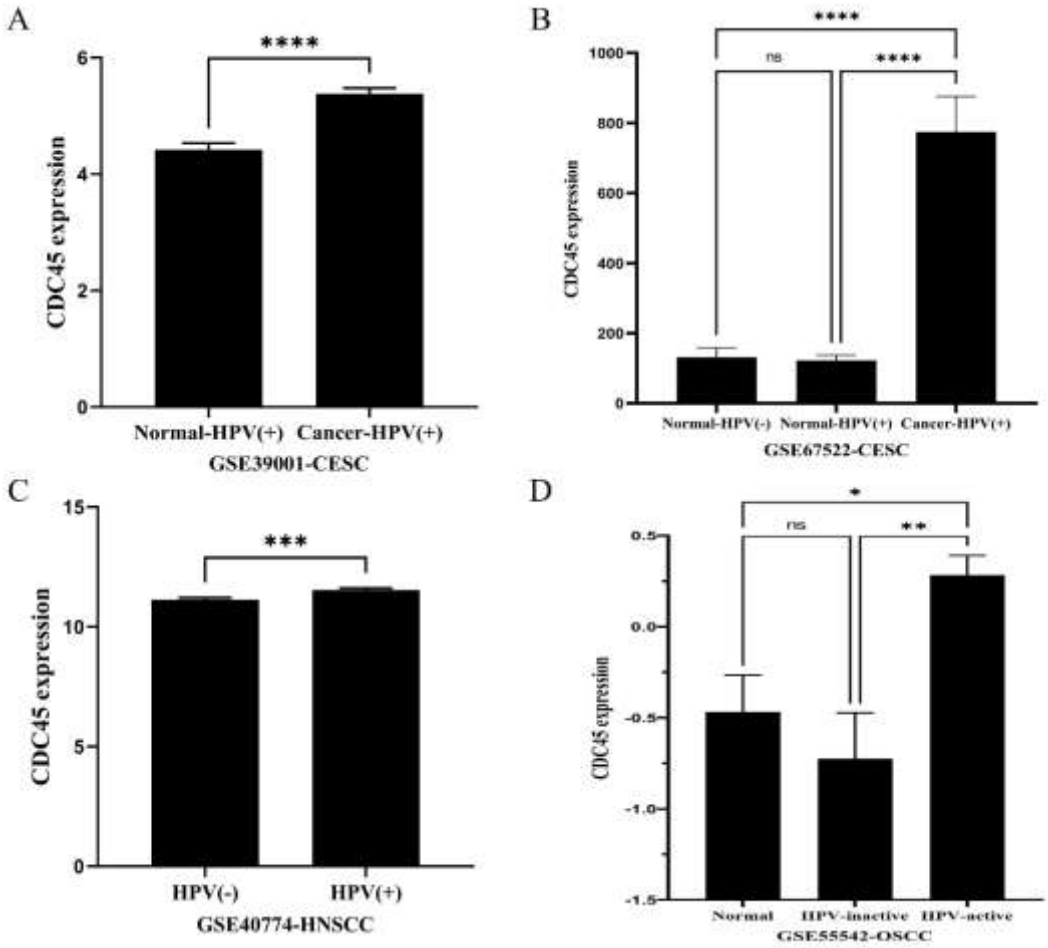

Figure 3, CDC45 expression in HPV-positive CC, HNSCC, OSCC and normal cervical tissues. (A-B) The expression of CDC45 in HPV-positive cervical cancer (CC) tissues, HPV-positive normal cervical tissues, and HPV-negative normal cervical tissues. C, The expression of CDC45 in HPV-positive head and neck squamous cell carcinoma (HNSCC) and normal tissues. (D): The expression of CDC45 in HPV-active and HPV-inactive in oral squamous cell carcinoma (OSCC) and normal tissues. (*, p < 0.05; **, p < 0.01; ***, p < 0.001; ****, p < 0.0001).

3.2 Protein-Protein Interaction Network Identification and Gene Set Enrichment Analysis of CDC45

GSEA in the TCGA-CESC dataset showed that CDC45 was significantly associated with various gene sets (Figure 4), including MISMATCH_ REPAIR (ES=0.8750, NP=0.0000), HOMOLOG OUS_RECOMBINATION (ES=0.8315, NP=0.0 000), BASE_EXCISION_REPAIR (ES=0.7509, NP=0.0000), DNA_REPLICATION (ES=0.9130, NP=0.0000), SPLICEOSOME (ES=0.7175, NP= 0.0000), NUCLEOTIDE_ EXCISION_ REPAIR (ES=0.7847, NP=0.0000), CELL_ CYCLE (ES= 0.7168, NP=0.0000), PYRIMIDINE _METAB OLISM (ES=0.6918, NP=0.0000), PROTEA SOME (ES=0.7233, NP=0.0000), and PURINE _METABOLISM (ES=0.5060, NP=0.0 000).

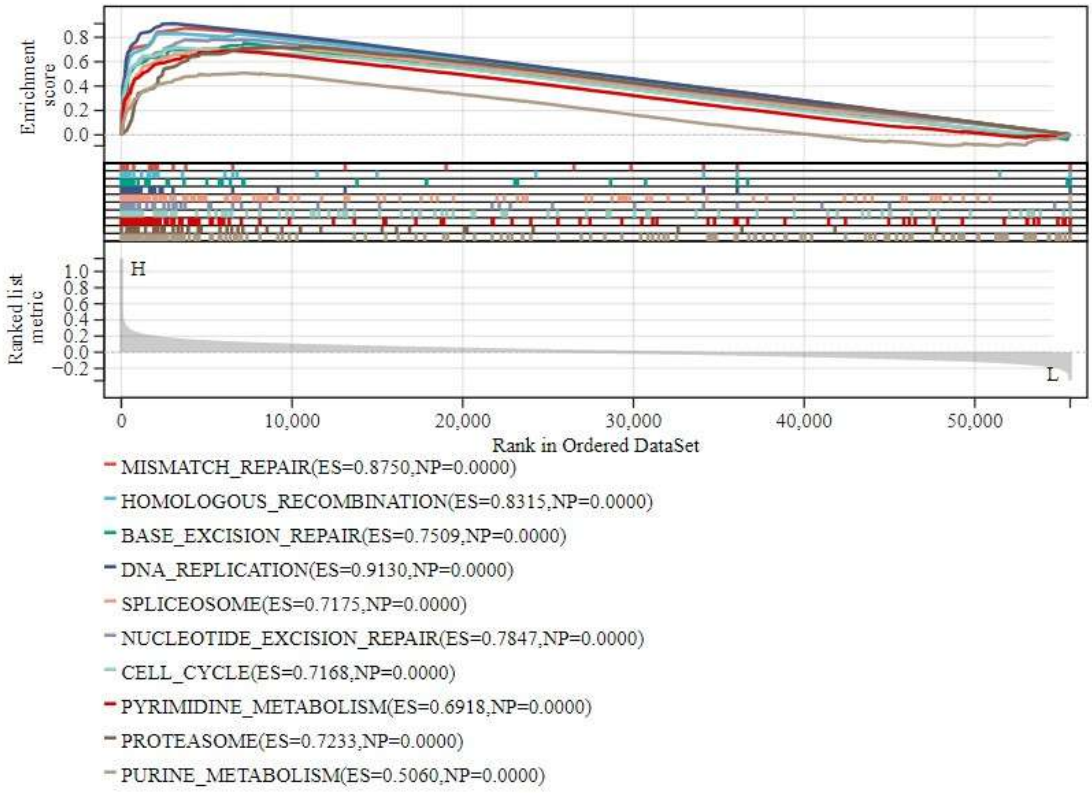

Figure 4, Gene set enrichment analysis of CDC45 in CC in the TCGA-CESC dataset.

3.3 CDC45 Impacted the Prognosis and Established a Clinical Prediction Model in Cervical Cancer

OS and PFS were significantly longer in patients with CC in the high-CDC45-expression group than in those in the low-CDC45-expression group in the TCGA-CESC dataset, (p = 0.022, HR (High group) =0.580, 95%CI (0.363-0.924) and p = 0.016, HR (High group) =0.563, 95%CI (0.353-0.897); Figures 5 A–B). Univariate and multivariate Cox regression analyses of OS in the TCGA-CESC dataset were performed with *CDC45*, age, pathological tumor-node-metastasis (p-TNM) stage, tumor grade, and smoking as variables. The univariate and multivariate Cox analysis revealed significant differences in OS related to *CDC45* (univariate Cox analysis: p=0.025, HR=0.623 [95%CI, 0.412 - 0.943]; multivariate Cox analysis: *CDC45*, p=0.033, HR=0.636 [95% CI, 0.420 - 0.964]) and p-TNM stage (I vs IV) (univariate Cox analysis: p < 0.001, HR=6.039 [95% CI, 2.549 - 14.309]; multivariate Cox analysis: p < 0.001, HR=5.971 [95% CI, 2.523 - 14.131]); Table 2). Accordingly, *CDC45* and p-TNM stage (I vs IV) (p<0.05) were selected as factors to establish a prognostic nomogram for the TCGA-CESC dataset. The total points ranged from 0 to 180, and the C-index value was 0.702 (95% CI, 0.573−0.831; p = 0.002; Figure 5 C). The nomogram can predict the 1-year, 3-year, and 5-year overall survival of CC patients (Figure 5 D).

Table 2, Univariate and multivariate Cox regression analyses of OS in the TCGA-CESC dataset

Variables	**Univariate**		**Multivariate**	
	p	HR (95%CI)	p	HR (95%CI)
CDC45	0.025	0.623 (0.412 - 0.943)	0.033	0.636 (0.420 - 0.964)
Age	0.289	1.012 (0.990 - 1.035)		
Grade				
G1 vs G3-4	0.498	1.536 (0.445 - 5.307)		

G2 vs G3-4	0.783	1.092 (0.586 - 2.035)		
p-TNM stage				
II vs I	0.392	0.689 (0.294 - 1.617)		
III vs I	0.212	1.611 (0.762 - 3.408)		
IV vs I	< 0.001	6.039 (2.549 - 14.309)	＜0.001	5.971 (2.523 - 14.131)
Smoking (No vs Yes)	0.393	1.292 (0.717 - 2.328)		

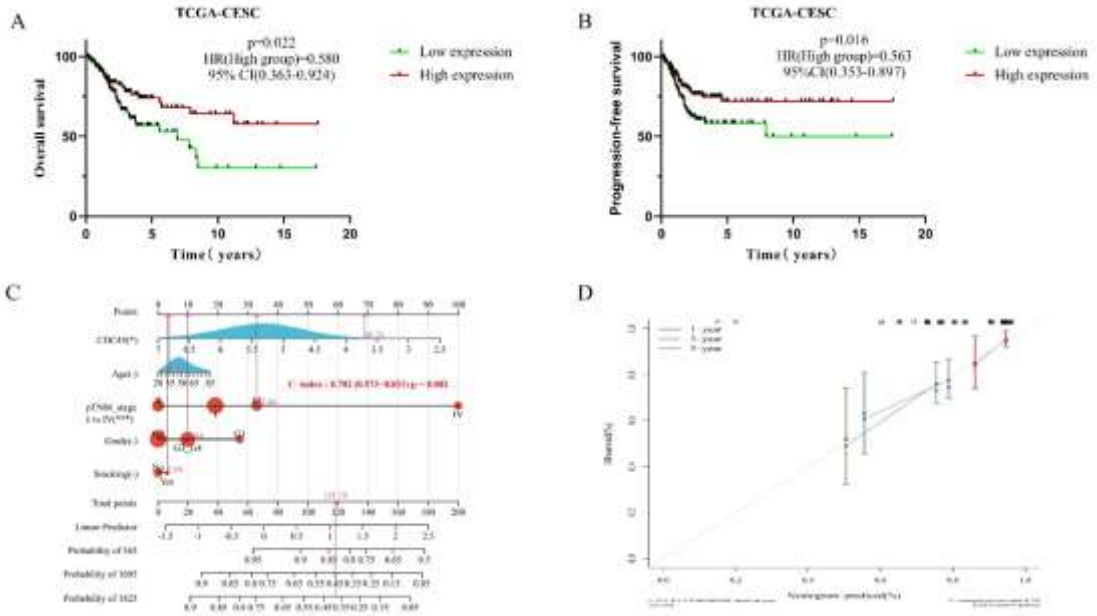

Figure 5, Effects of CDC45 on the prognosis and established a clinical prediction model in CC. (A–B) The expression of CDC45 affected OS and PFS in CC. (C) *CDC45* and p-TNM stage were selected as factors to establish a prognostic nomogram for the TCGA-CESC dataset. (D)The nomogram can predict the 1-year, 3-year, and 5-year overall survival of CC patients.

3.4 The Expression and Prognosis Of CDC45 in Pan-Cancer

CDC45 is lowly expressed in TCGA-TCGT dataset (p＜0.0001, Figure 6 A), while it is overexpressed in other tumors (p＜0.01, Figure 6 A). Low expression of CDC45 was correlated with a poor prognosis in the TCGA-DLBC (N = 44, p = 9.4e-3, HR = 0.33 [0.14, 0.81]), TCGA-CESC (N = 273, p =0.01, HR = 0.64 [0.45, 0.91]), TCGA-THYM (N = 117, p =0.01, HR = 0.67 [0.47, 0.95]), and TCGA-OV (N = 407, p = 0.02, HR = 0.88 [0.79, 0.98]) datasets (Figure 6 B). On the contrary, high expression of CDC45 was correlated with a poor prognosis in the TCGA-GBMLGG, TCGA-KIPAN, TCGA-LGG, TCGA-ACC, TCGA-MESO, TCGA-KIRC, TCGA-LIHC, TCGA-KICH, TCGA-KIRP, TCGA-LUAD, TCGA-PAAD, TCGA-LAML, TCGA-UVM, TCGA-SARC, TARGET-ALL-R, TARGET-LAML, and TCGA-SKCM datasets (Figure 6 B and Table 3).

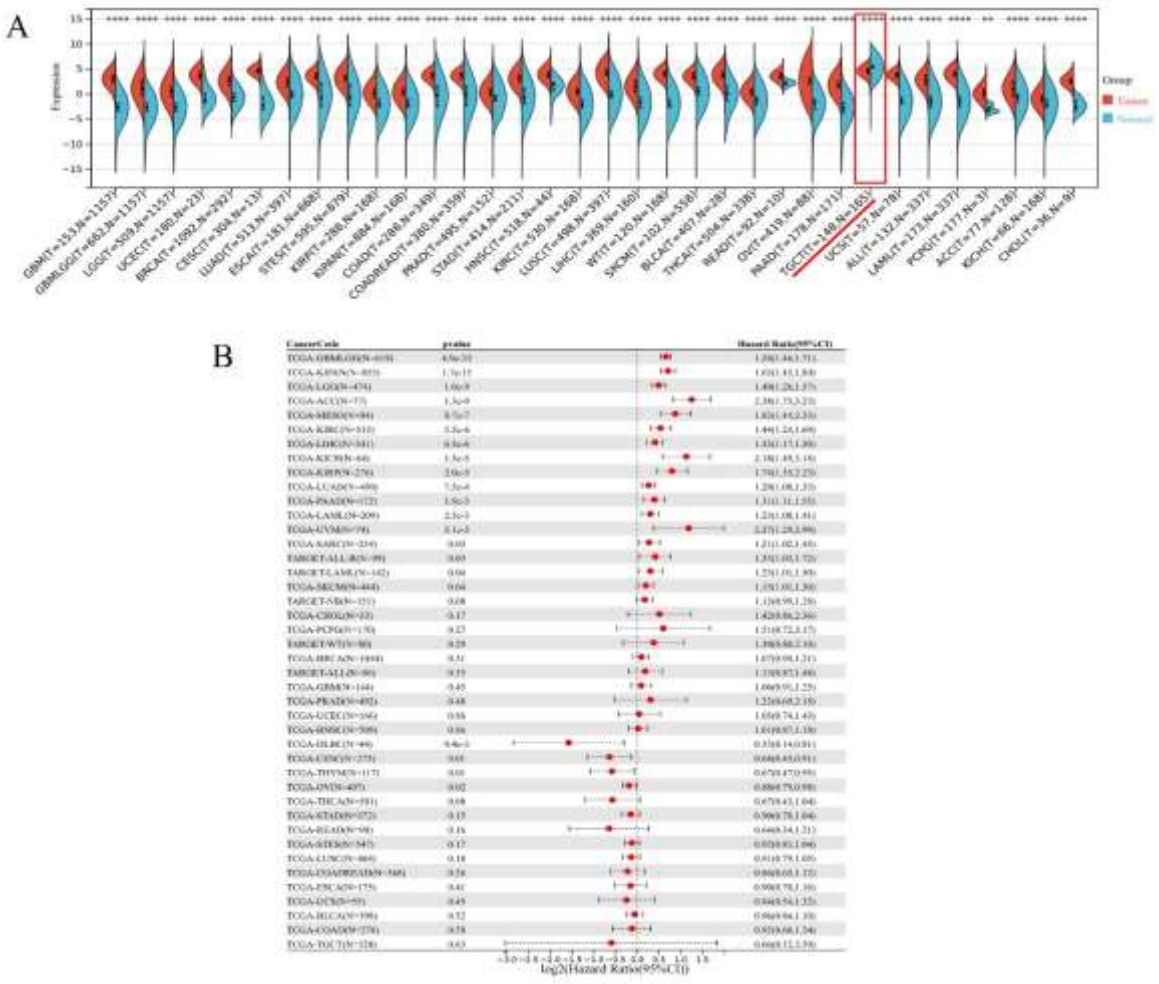

Table 3, The differences in prognosis between CDC45 and pan cancer.

Cancer types	Abbreviations	N	P	Hazard Ratio(95%CI)
Glioma	TCGA-GBMLGG	619	4.9e-33	1.58(1.46,1.71)
Pan-kidney cohort (KICH+KIRC+KIRP)	TCGA-KIPAN	855	1.7e-15	1.63(1.45,1.84)
Brain Lower Grade Glioma	TCGA-LGG	474	1.0e-9	1.40(1.26,1.57)
Adrenocortical carcinoma	TCGA-ACC	77	1.3e-9	2.38(1.75,3.23)
Mesothelioma	TCGA-MESO	84	8.7e-7	1.83(1.44,2.33)
Kidney renal clear cell carcinoma	TCGA-KIRC	515	5.5e-6	1.44(1.24,1.69)
Liver hepatocellular carcinoma	TCGA-LIHC	341	6.3e-6	1.33(1.17,1.50)
Kidney Chromophobe	TCGA-KICH	64	1.5e-5	2.18(1.49,3.18)
Kidney renal papillary cell carcinoma	TCGA-KIRP	276	2.0e-5	1.74(1.35,2.23)
Lung adenocarcinoma	TCGA-LUAD	490	7.5e-4	1.20(1.08,1.33)
Pancreatic adenocarcinoma	TCGA-PAAD	172	1.9e-3	1.31(1.11,1.55)
Acute Myeloid Leukemia	TCGA-LAML	209	2.5e-3	1.23(1.08,1.41)
Uveal Melanoma	TCGA-UVM	74	5.1e-3	2.27(1.29,3.99)
Sarcoma	TCGA-SARC	254	0.03	1.21(1.02,1.43)
Acute Lymphoblastic Leukemia	TARGET-ALL-R	99	0.03	1.33(1.03,1.72)
Acute Myeloid Leukemia-like	TARGET-LAML	142	0.04	1.23(1.01,1.50)
Skin Cutaneous Melanoma	TCGA-SKCM	444	0.04	1.15(1.01,1.30)

4. Discussion

CC pathogenesis is predominantly driven by persistent high-risk human papillomavirus (HR-HPV) infection, which accounts for approximately 95% of cases [16]. HR-HPV exerts its oncogenic effects primarily through viral proteins E6 and E7, which inactivate tumor suppressors p53 and pRb, respectively [17]. Among HR-HPV subtypes, HPV16 poses the highest risk, being implicated in ~50% of CC cases [16,17].

In this study, we demonstrated that CDC45 expression was significantly elevated in CC tissues compared to normal controls ($p<0.0001$). Notably, while HPV-positive normal cervical tissues exhibited baseline CDC45 levels comparable to those of HPV-negative counterparts, CDC45 overexpression was specifically amplified during HPV-associated malignant transformation. This expression pattern extends beyond CC, as pan-cancer analyses revealed CDC45 dysregulation across multiple malignancies, correlating with divergent prognostic outcomes depending on tumor type.

As a core member of the DNA replication initiation complex, CDC45 overexpression may promote tumor cell proliferation by accelerating the cell cycle progression [18]. In gastric cancer, both mRNA and protein expression levels of CDC45 are significantly higher in tumor tissues than adjacent normal tissues. The diagnostic efficacy was evaluated by ROC curve analysis, with an AUC value above 0.8, indicating the potential of CDC45 as a novel diagnostic biomarker for gastric cancer [19]. In breast cancer (MCF-7) and lung cancer (H1299) cell lines, CDC45 expression levels are positively correlated with cell proliferation, and inhibition of its expression significantly reduces tumor cell viability [20-21]. CDC45 is overexpressed in colorectal cancer (CRC) tissues and may be associated with TNM staging, lymph node metastasis, and distant metastasis. High CDC45 expression correlates with better PFS and OS, suggesting its potential as a diagnostic, therapeutic, and prognostic target for CRC [22]. In non-small cell lung cancer (NSCLC), CDC45 overexpression in tumor tissues is closely related to advanced tumor staging and lymph node metastasis. Moreover, CDC45 serves as a prognostic risk factor (HR>1, $p<0.05$) [23]. He et al. [24] found that CDC45 was overexpressed in cervical cancer tissues and significantly associated with advanced FIGO staging, lymph node metastasis, and poor survival, which is consistent with our results.

In this study, we performed enrichment analysis of CDC45 in CC using TCGA database. We found a significant correlation between CDC45 and mismatch repair (MMR), homologous recombination, DNA replication, and the cell cycle. The MMR system is a crucial repair mechanism in DNA replication, responsible for correcting base pairing errors and maintaining genomic stability [25]. Its functional defects may lead to microsatellite instability (MSI) and accumulation of gene mutations, thereby increasing tumor risk [25-26]. Chung et al. [27] studied MSI in 50 cervical cancer cases and found that patients with MSI-high tumors exhibited lower overall survival, suggesting that MMR deficiency may contribute to tumor progression and poor prognosis in CC.

Defects in the MMR system leaded to MSI, which prevents DNA replication errors from being repaired and results in mutations in oncogenes (such as, HER2) and tumor suppressor genes (e.g., TP53) [28]. For example, TP53 mutations are common in cervical cancer and may promote carcinogenesis by dysregulating the cell cycle and apoptosis [29]. Tumors with MMR deficiency often exhibit high tumor mutation burden (TMB), which may enhance response to immunotherapy [30]. Research has shown that detecting PD-L1 and MMR status can help identify cervical cancer patients who may benefit from immune checkpoint inhibitors [31]. Therefore, MMR system defects promote cervical carcinogenesis by inducing genomic instability and mutagenesis.

The biological function of CDC45 is closely related to cell cycle checkpoints (e.g., the S phase and G2/M phase checkpoints), and its abnormal expression may lead to genomic instability and tumorigenesis [32-33]. Abnormal CDC45 expression or functional defects can lead to replication fork arrest, activate the ATR/CHK1 signaling pathway, and trigger S phase checkpoint activation. Studies have shown that CDC45 overexpression may induce genomic instability and increase tumor risk by accelerating replication

fork elongation [33-34]. CDC45 is significantly upregulated in multiple cancers, including colorectal and hepatic malignancies, and is associated with poor patient prognosis. The underlying mechanism may involve E2F transcription factor-mediated cell cycle progression and suppression of p53-dependent G1 checkpoint function, enabling sustained proliferation of DNA-damaged cells [35-36].

However, this study has its limitations. Such as the functional validation of CDC45's biological role in CC models remains pending, necessitating future siRNA/CRISPR-mediated knockdown experiments. In addition, our clinical cohort size (n=6 tumor-normal pairs) limits statistical power for subgroup analyses. Nevertheless, multi-cohort bioinformatics validation (TCGA/GEO) coupled with orthogonal qPCR/WB confirmation strengthens the reliability of CDC45's overexpression pattern. CDC45 significantly impacts the prognosis of cervical cancer (CC). Notably, its expression is closely associated with diverse malignancies, particularly HPV-associated tumors. In addition, CDC45 demonstrates prognostic relevance across multiple cancer types.

Acknowledgments: Not applicable.

Funding: No funding.

Institutional Review Board Statement: Not Applicable

Conflict of Interest Statement: The authors declare no potential conflicts of interest.

Authors Contributions

Q.M. and X.Z. conceived and designed the project. X.H. and B.L. acquired, analyzed, and interpreted the data. All authors wrote and revised the paper.

Ethics Approval And Consent To Participate

The protocol and methodology of the present study were approved by the Ethics Committee of Zhuzhou Central Hospital (No. 20231046).

Reference

1. Li T, Zhang H, Lian M, et al. Global status and attributable risk factors of breast, cervical, ovarian, and uterine cancers from 1990 to 2021. J Hematol Oncol. 2025;18(1):5.
2. Yuan M, Zhao X, Wang H, Hu S, Zhao F. Trend in Cervical Cancer Incidence and Mortality Rates in China, 2006-2030: A Bayesian Age-Period-Cohort Modeling Study. Cancer Epidemiol Biomarkers Prev. 2023;32(6):825-833.
3. Han B, Zheng R, Zeng H, et al. Cancer incidence and mortality in China, 2022. J Natl Cancer Cent. 2024;4(1):47-53.
4. American Cancer Society, Cervical Cancer. cancer.org | 1.800.227.2345. https://www.cancer.org/content/dam/CRC/PDF/Public/8599.00.pdf.
5. National Cancer Institute: Cancer Stat Facts: Cervical Cancer. https://seer.cancer.gov/statfacts/html/cervix.html.
6. Okunade KS. Human papillomavirus and cervical cancer [published correction appears in J Obstet Gynaecol. 2020 May;40(4):590.
7. Van Gerwen OT, Muzny CA, Marrazzo JM. Sexually transmitted infections and female reproductive health. Nat Microbiol. 2022 Aug;7(8):1116-1126.
8. Mabuchi, S., Kawano, M., Sasano, T., Kuroda, H. (2023). Management of Early-Stage and Locally Advanced Cervical Cancer. In: Shoupe, D. (eds) Handbook of Gynecology. Springer, Cham. https://doi.org/10.1007/978-3-031-14881-1_34
9. Musunuru HB, Pifer PM, Mohindra P, Albuquerque K, Beriwal S. Advances in management of locally advanced cervical cancer. Indian J Med Res. 2021;154(2):248-261.
10. Briu LM, Maric C, Cadoret JC. Replication Stress, Genomic Instability, and Replication Timing: A Complex Relationship. Int J Mol Sci. 2021 Apr 30;22(9):4764.
11. Petojevic T, Pesavento JJ, Costa A, et al. Cdc45 (cell division cycle protein 45) guards the gate of the Eukaryote Replisome helicase stabilizing leading strand engagement. Proc Natl Acad Sci U S A. 2015;112(3):E249-E258.
12. Fu Y, Lv Z, Kong D, Fan Y, Dong B. High abundance of CDC45 inhibits cell proliferation through elevation of HSPA6. Cell Prolif. 2022;55(7):e13257.
13. Lian YF, Li SS, Huang YL, et al. Up-regulated and interrelated expressions of GINS subunits predict poor prognosis in hepatocellular carcinoma. Biosci Rep. 2018;38(6):BSR20181178.
14. Zhang JN, Li LW, Cao MQ, et al. Functional

Analysis and Experimental Validation of the Prognostic and Immune Effects of the Oncogenic Protein CDC45 in Breast Cancer. Breast Cancer (Dove Med Press). 2025;17:11-25.
15. Nepon-Sixt BS, Bryant VL, Alexandrow MG. Myc-driven chromatin accessibility regulates Cdc45 assembly into CMG helicases. Commun Biol. 2019;2:110.
16. Okunade KS. Human papillomavirus and cervical cancer. J Obstet Gynaecol. 2020 Jul; 40(5):602-608.
17. Zhang Y, Qiu K, Ren J, Zhao Y, Cheng P. Roles of human papillomavirus in cancers: oncogenic mechanisms and clinical use. Signal Transduct Target Ther. 2025;10 (1):44.
18. Radhakrishnan A, Sharma C, Malviya VN, Srivastav R. Deciphering the molecular functionality of Cdc45 in replisomal complex. Biochem Biophys Rep. 2024;37:101 643.
19. Wu L, Gao G, Mi H, et al. Validation of CDC45 as a novel biomarker for diagnosis and prognosis of gastric cancer. PeerJ. 2024; 12:e17130.
20. Zhang JN, Li LW, Cao MQ, et al. Functional Analysis and Experimental Validation of the Prognostic and Immune Effects of the Oncogenic Protein CDC45 in Breast Cancer. Breast Cancer (Dove Med Press). 2025;17:11-25.
21. Fan YL, Liu RJ, Ding XY, Shangguan XY, Wu XR. Nan Fang Yi Ke Da Xue Xue Bao. 2017;37(11):1545-1550.
22. Hu Y, Wang L, Li Z, et al. Potential Prognostic and Diagnostic Values of CDC6, CDC45, ORC6 and SNHG7 in Colorectal Cancer. Onco Targets Ther. 2019;12:11609-11621.
23. He Z, Wang X, Yang Z, et al. Expression and prognosis of CDC45 in cervical cancer based on the GEO database. PeerJ. 2021;9:e12114.
24. Li GM. Mechanisms and functions of DNA mismatch repair. Cell Res. 2008;18(1):85-98.
25. Yamamoto H, Watanabe Y, Arai H, Umemoto K, Tateishi K, Sunakawa Y. Microsatellite instability: A 2024 update. Cancer Sci. 2024 ;115(6):1738-1748.
26. Chung TK, Cheung TH, Wang VW, Yu MY, Wong YF. Microsatellite instability, expression of hMSH2 and hMLH1 and HPV infection in cervical cancer and their clinico-pathological association. Gynecol Obstet Invest. 2001;52(2):98-103.
27. Huang Y, Li GM. DNA mismatch repair in the context of chromatin [published correction appears in Cell Biosci. 2020 Jul 2;10:84.
28. Zhao X, Sun W, Ren Y, Lu Z. Therapeutic potential of p53 reactivation in cervical cancer. Crit Rev Oncol Hematol. 2021;157: 103182.
29. Westcott PMK, Muyas F, Hauck H, et al. Mismatch repair deficiency is not sufficient to elicit tumor immunogenicity. Nat Genet. 2023;55(10):1686-1695.
30. Guo F, Lu R, Kong W, Anwar M, Feng Y. DNA mismatch repair system regulates the expression of PD-L1 through DNMTs in cervical cancer. Cancer Cell Int. 2024;24(1): 25.
31. Broderick R, Nasheuer HP. Regulation of Cdc45 in the cell cycle and after DNA damage. Biochem Soc Trans. 2009;37(Pt 4):926-930.
32. Fu Y, Lv Z, Kong D, Fan Y, Dong B. High abundance of CDC45 inhibits cell proliferation through elevation of HSPA6 . Cell Prolif. 2022;55(7):e13257.
33. Radhakrishnan A, Sharma C, Malviya VN, Srivastav R. Deciphering the molecular functionality of Cdc45 in replisomal complex. Biochem Biophys Rep. 2024;37: 10 1643.
34. Yang S, Ren X, Liang Y, et al. KNK437 restricts the growth and metastasis of colorectal cancer via targeting DNAJA1/ CDC45 axis. Oncogene. 2020;39(2):249-261.
35. Lu HP, Du XF, Li JD, et al. Expression of Cell Division Cycle Protein 45 in Tissue Microarrays and the CDC45 Gene by Bioinformatics Analysis in Human Hepatocellular Carcinoma and Patient Outcomes. Med Sci Monit. 2021;27:e928800.